IEEE Access
Multidisciplinary : Rapid Review : Open Access Journal

Received 3 October 2022, accepted 12 October 2022, date of publication 17 October 2022, date of current version 24 October 2022.

Digital Object Identifier 10.1109/ACCESS.2022.3215080

RESEARCH ARTICLE

Probabilistic LSTM-Autoencoder Based Hour-Ahead Solar Power Forecasting Model for Intra-Day Electricity Market Participation: A Polish Case Study

VISHNU SURESH [1], (Member, IEEE), **FACHRIZAL AKSAN** [1], (Student Member, IEEE), **PRZEMYSLAW JANIK** [1], **TOMASZ SIKORSKI** [1], (Member, IEEE), AND **B. SRI REVATHI** [2]

[1]Faculty of Electrical Engineering, Wroclaw University of Science and Technology, 50370 Wroclaw, Poland
[2]School of Electrical Engineering, Vellore Institute of Technology, Chennai 600127, India

Corresponding author: Vishnu Suresh (vishnu.suresh@pwr.edu.pl)

This work was supported by The National Centre for Research and Development in Poland related to the project ''Multi Energy Storage Hub For reliable and commercial systems Utilization'' (MESH4U), through the European Research Area Networks (ERA-NET) Smart Energy System, ERA-NET Smart Grids Plus Joint Call 2019 on Energy Storage Solutions (MICall2019), European SET-Plan Action 4 ''Increase the resilience and security of the energy system,'' under Contract SMARTGRIDSPLUS/4/5/MESH4U/2021.

ABSTRACT This article presents the selection of an appropriate deep learning Long Short-Term Memory (LSTM) based probabilistic hour-ahead forecasting model for a grid connected industrial solar PV power plant located in Poland. It has a 317 kW peak power capacity and is connected with a metallurgical plant producing steel for car parts. The purpose of the study is to present a model that could be used by the plant to participate in the Polish intra-day electricity market. Four different LSTM models were investigated which include the vanilla model, the stacked LSTM model, the Bi-directional LSTM model and the LSTM-Autoencoder model. Out of the investigated models it was observed that the LSTM-Autoencoder model was the best performing one in terms of reliability. The average Root Mean Squared Error (RMSE) and the average Mean Absolute Error (MAE) for the Autoencoder model over 100 runs were 15.59 kW and 8.36 kW which represent 4.9% and 2.6% of the peak power respectively. Moreover, it was observed that it has the shortest width for the 95% confidence interval of only 0.5% for both the RMSE and the MAE. In terms of accuracy the best performing model was the LSTM bi-directional model with the average RMSE and MAE values of 12.87 kW and 6.91 kW which represent 4% and 2.1% of the peak power. The 95% confidence intervals width for both the RMSE and MAE over the 100 runs were 0.8% and 0.5% respectively.

INDEX TERMS Solar power forecasting, LSTM, deep learning, electricity market and grid connected solar PV.

I. INTRODUCTION

In the current political scenario, there is a considerable driving force for the adoption of renewable sources of energy and within them solar photovoltaics. The European Green deal as laid down by the European commission stipulates that in order to reduce emissions by 55%, 21-22 GW of Photovoltaics (PV) has to be added annually. Moreover, if the emissions need to be reduced by 60% this amount has to be increased by another 5-10 GW [1], [2].

Due to the developments stated above, as the installed capacity of renewable energy increases so does their participation in the electricity markets. In this paper a case study is presented wherein the objective was to develop a short-term probabilistic forecasting model for an industrial solar pv plant of 317 kW peak power so that the operator of the plant could participate in the hour-ahead intra-day settlements. The rationale behind choosing LSTM models

The associate editor coordinating the review of this manuscript and approving it for publication was Fabio Mottola.

over others and the literature review for the study is presented below.

In order to select the right forecasting approach, a search was made in the Web of Science covering all databases with the keywords "Short term solar forecasting review". From the presented results a mix of both recent and highly cited articles were selected [3], [4], [5]. While a number of options were available such as sky cameras based, satellite based, LIDAR based, statistical methods, decompositions based and machine learning based techniques. It was seen that the LSTM was common to all the review papers, it was also mentioned that it was a powerful tool for handling time series data and to characterize the temporal dependencies within the data.

A. LITERATURE REVIEW: SIMPLE LSTM AND RNN-LSTM MODELS

While the review papers revealed that the LSTM model is a good fit for short-term forecasts it was noticed in the literature review that there are numerous architectures of the LSTM model which could be used. A number of both recent and highly cited papers were selected from the results obtained by searching for "LSTM hour ahead solar forecasting" in the Web of Science. Analysis of the different LSTM models used are as follows. A simplified model consisting of a single LSTM layer with 30 cells and a dense layer with one neuron is presented in [6]. The dataset considered for this study was obtained from the island of Santiago, Cape Verde. Since the irradiation was not available at the location, weather forecasting data was instead used to predict the solar irradiation at the hour-ahead time horizon. The input dataset considered numerous variables such as the hour, day, and month of the day under consideration along with other weather dependent factors such as temperature, dew point, humidity, visibility, wind speed and weather type. The performance of the proposed model on the indicated dataset was compared with other models such as the persistence model, linear least square regression model and the regular feed-forward neural network with back propagation. It was seen that the LSTM model was 18.34% more accurate in terms of point forecasts made by the second best neural network model.

A study that conducted hour-ahead forecasting for 3 different solar panel technologies is presented in. [7]. This included the monocrystalline technology, thin-film technology, and the polycrystalline technology. The dataset under consideration was hourly recorded over 4 years and was obtained from the solar panels located at the university of Malaya. The variables considered were solar radiation, wind speed, temperature. The study proposed an RNN-LSTM method for the forecasts and evaluated its performance against a number of methods such as regression-based models, hybrid ANFIS models and machine learning models such as Artificial Neural Networks (ANN) and Support Vector Machines (SVM). The evaluation metrics used were the Root Mean Squared Error (RMSE), Mean Squared Error (MSE) and Mean Absolute Error (MAE). The proposed model outperformed other models with a low RMSE value of 26.85 W/m^2, 39.2 W/m^2 and 19.78 W/m^2 for the above mentioned 3 solar panel technologies respectively.

B. LITERATURE REVIEW: CNN-LSTM AND LSTM BI-DIRECTIONAL MODELS

A very-short term intra hour 10 minutes ahead forecasting of solar irradiation by using a combination of total sky images and historical data is presented in [8]. The proposed model is a Siamese Convolutional Neural Network – Long Short-Term Memory (SCNN – LSTM). The data used was obtained from National Renewable Energy Laboratory (NREL)'s solar radiation facility in Golden City, Colorado spanning 2 years. The performance of the model was compared against several others such as the Multi-Layer Perceptron (MLP) model, regular LSTM model, SolarNet and 3D – CNN model. The model results for comparison were taken from the literature and it was shown that the SCNN-LSTM achieved a Normalized – RMSE of 23.47% and a forecast skill of 24.51% and outperformed the other models.

Solar irradiance forecasting using a bi-directional LSTM model along with wavelet decomposition is proposed in [9]. The process involves forecasting for every decomposed frequency feature and the final point forecast produced as a result of reconstruction using the wavelet decomposition technique. The RMSE, MAE, MAPE, coefficient of determination and the forecasting skill were used to compare its performance with gated recurrent unit model, LSTM model and a naïve baseline model. The results show the superiority of the bi-directional model used with wavelet decomposition. Other highly cited articles on the topic are as follows, in [10] a Support Vector Machine (SVM) based on Genetic Algorithm (GA) for short term solar power output forecasting in a residential area is provided which shows an improvement of 98.76% in terms of the MAPE. A comprehensive review paper that analyses numerous solar PV power forecasting manuscripts can be found in [11]. It discusses the role of correlation between the features and the outputs in forecasting and also the performances of both conventional statistical and intelligent machine learning algorithms. Finally, it highlights the importance of optimization in utilizing different forecasting models. A Differential Evolution Particle Swarm Optimization (DEPSO) based forecasting model for short term PV output power forecasting for a system located in Deakin University, Victoria, Australia is described in [12]. The results of this approach have been compared with Particle Swarm Optimization (PSO) and Differential Evolution (DE) optimized forecasting models and the proposed DEPSO shown a significant improvement in the accuracy metrics used. The motivation for this research and research article is as follows:

- Lack of sufficient probabilistic forecasts by deep learning-based models in the literature. In fact, a search of "Probabilistic LSTM solar forecasting" on the web of

science resulted only in 2 publications that were relevant to this context.
- Uncertain forecast requirements by the company participating in the electricity market for better decision making.
- Selection of the right LSTM architecture from the most popular options for short term solar power output forecasts.

The technical contribution of the paper are as follows:
- Probabilistic-interval forecasts are made using the LSTM-Autoencoder model which improves the decision-making process for the user by providing best- and worst-case generation scenarios.
- Comparison of 4 different LSTM architectures which according to the knowledge of the authors have not been compared yet in the literature.
- An hour ahead solar power forecasting system for a grid connected PV system for this particular region of Poland.

The rest of the paper is organized as follows. Section 2 presents 4 different LSTM architectures that were considered in the study and their architecture optimzation. Section 3 presents the data and the data processing techniques that were used in the study. Section 4 presents the evaluation metrics that were used to compare the different models that were investigated. Section 5 presents the results and their interpretation and analysis. Finally, the paper is concluded followed by references.

II. LSTM ARCHITECTURES

The LSTM cell and its structure has already been discussed in detail by the authors in [13]. The comparison of its structure and mathematical model with the RNN structure is also provided in the article. Moreover, it is a topic that is covered extensively in the literature and can also be found in [6] and [14].

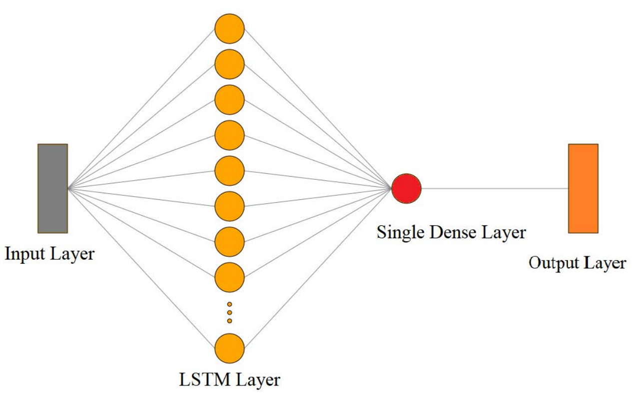

FIGURE 1. **Vanilla LSTM architecture.**

A. VANILLA LSTM MODEL

The Vanilla LSTM model is a simple but quick and effective model. It has been used extensively for forecasting purposes of not only solar output powers/irradiation but also other applications. It's structure in general is elaborated in [6], [15], and [16] and for this study the structure used is shown in Fig. 1 and explained as follows.

The input layer of the structure is in a 3-Dimensional format [samples, timesteps, features]. This data is then fed into an LSTM layer that consists of 4 cells that ascertain the temporal relationship present within the data. This is then followed by the Single Dense Layer which is a regular neural network cell and an output layer to make a prediction based on the learned representations by the LSTM layer.

B. BI-DIRECTIONAL LSTM MODEL

The bi-directional LSTM model learns the temporal relationship embedded within the data in a forward and backward direction. This means that given a vector of inputs to the model it is able to understand the relationship between the past and future samples moving from both the past to future direction and from the future to past direction. Such models have been implemented in the studies [9], [17] and in this study the following architecture with the bi-directional LSTM layer is shown in Fig. 2.

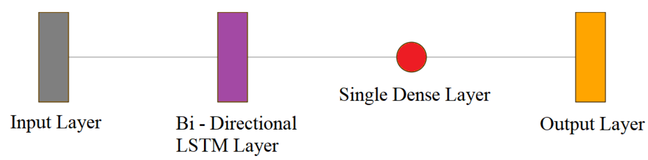

FIGURE 2. **Bi-directional LSTM architecture.**

The input, output and the single dense layer for this architecture are the same as for the vanilla model. The key difference is the bi-directional LSTM layer which as mentioned earlier scans for the temporal dependencies within the data in two directions compared to the one direction in the vanilla LSTM layer.

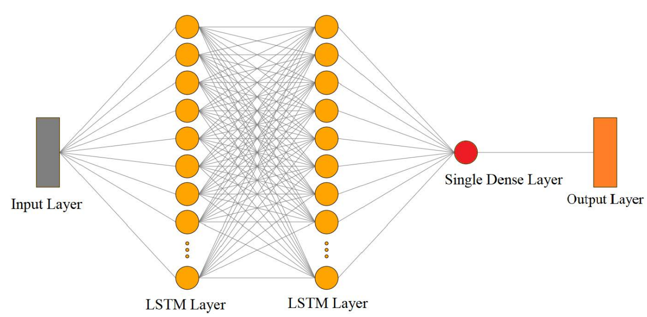

FIGURE 3. **Stacked LSTM architecture.**

C. STACKED LSTM MODEL

The stacked LSTM model is a heavier version of the simple vanilla model and is more effective in learning complex temporal dependencies [18], [19]. The stacked LSTM structure used in this study is shown in Fig. 3. The distinguishing feature of this model is the presence of 2 LSTM layers each containing 5 cells. The first layer presents vectors of learned representations based on the data from the input layer. This is further used by the next layer to extract more complex relationships based on the data from the first layer. Finally, the single dense layer and the output layer together make the predictions.

D. LSTM AUTOENCODER MODEL

The LSTM Autoencoder model used in this study is shown in Fig. 4. The defining layers of this model are the encoder, decoder and the repeate vector. The encoder part of the model creates a learned representation from the input data in the form of a vector within which exist the complex dynamics of the temporal representations.

At this point the dimensions of the data are reduced and a compressed version is produced which can also be used with other machine/deep learning algorithms. This encoded vector is then passed on to the decoder via the repeat vector and the model's performance depends upon the effectiveness of the decoder to recreate the input vector as accurately as possible [13], [20]. In the model used in this study both the encoder and decoder consist of 3 cells each.

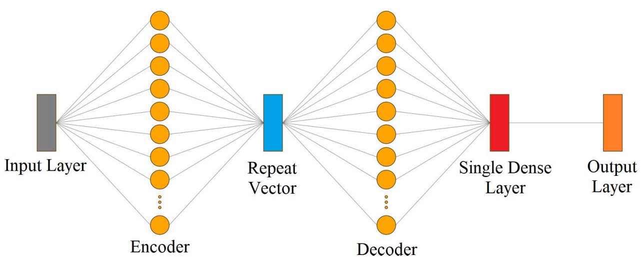

FIGURE 4. LSTM autoencoder architecture.

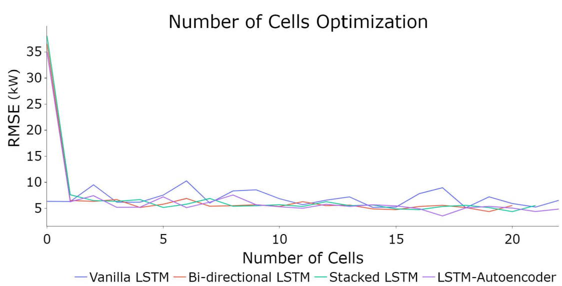

FIGURE 5. Number of cells optimization.

E. ARCHITECTURE OPTIMIZATION

Fig. 5 plots the RMSE on the test data for all considered architectures in terms of the number of cells used in the LSTM layers. It can be seen that for layers consisting of only 1 cell the RMSE remains quite high for all architectures and then it remains lower and stabilizes. For the Vanilla LSTM the number of cells with the best performance was 4. The number of cells in the LSTM layer for the Bi-directional model are also 4. The stacked model in each of its layer has 5 cells and finally the LSTM Autoencoder model has 3 cells.

In order to choose the right activation function, loss function and optimizer for each of the models the RMSE was evaluated for every combination of the above 3 parameters. The activation function was chosen amongst ReLu, sigmoid, softmax and tanh functions. The loss function was chosen amongst MSE, Mean Absolute Percentage Error (MAPE) and Mean Squared Logarithmic Error (MSLE). The optimizer was chosen amongst Adagrad, Adadelta, RMSprop and Adam. This resulted in a total of 48 combinations and the combination resulting in the lowest RMSE was chosen. In each case it was the ReLu activation function with the MSE loss function and Adam optimizer. The batch size used in this study is 24 taking into account the 24 hours prior to the forecast.

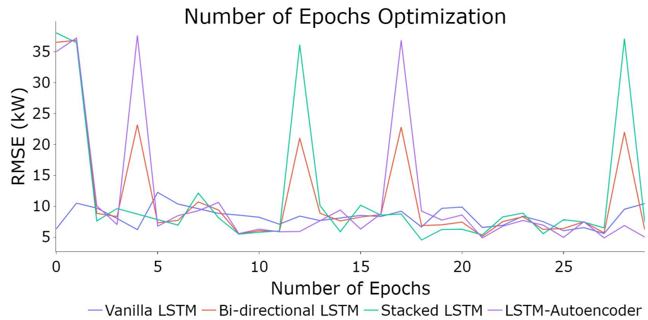

FIGURE 6. Number of epochs optimization.

Fig. 6 plots the RMSE as a function of the number of epochs for all the investigated models on the test dataset. It can be seen quite clearly that up to 5 epochs the RMSE remains quite high for all the models except the vanilla model and that after 5 epochs there are sporadic jumps to higher values during random epoch values. For the Bi-directional, Stacked and Autoencoder LSTM models the lowest RMSE at the earliest was observed with 9 epochs whereas for the vanilla model it was observed with 4 epochs. Hence, these epoch values are used to train the models.

III. DATA PREPROCESSING AND DESCRIPTION

A. IMPUTATION USING AUTO REGRESSIVE INTEGRATED MOVING AVERAGE MODEL (ARIMA)

The input data used in the study has missing values upto 0.5 % of its total data length. While such an amount is not significant it is imperative for deep learning models such as the LSTM to have as much data as possible. In fact, literature suggests that the performance of such models only improves with greater availability of data and computation performance [13], [21]. Hence, the ARIMA model was used to fill up the missing values. The method is well described in the literature [22], [23] and is described as follows. The model has three parts which are the Autoregressive (AR), Integrated (I) and Moving Average (MA) parts. In order to apply the ARIMA model the time series data under consideration should be stationary. In this study it was made possible by differencing the input data one time hence the value for I is 1. This was further confimed by using the Augumented Dickey Fuller (ADF) test that resulted in a p value The AR and MA values were determined using the PACF and ACF functions and have values of 2 and 1 respectively. Therefore, an ARIMA model of the order (2,1,1) was used. The time series values of the AR ($y_t^{\prime AR}$) and MA ($y_t^{\prime MA}$) parts are determined by equations (1) and (2).

$$y_t^{\prime AR} = \sum\nolimits_{i=1}^{m} \emptyset_i x_{t-i} + \omega_t = \emptyset_1 x_{t-1} + \emptyset_2 x_{t-2} + \ldots + \emptyset_m x_{t-m} + \omega_t \tag{1}$$

$$y_t^{\prime MA} = \sum\nolimits_{j=0}^{n} \theta_j \omega_{t-j} = \omega_t + \theta_1 \omega_{t-1} + \theta_2 \omega_{t-2} + \ldots + \theta_n \omega_{t-n} \tag{2}$$

where, $\emptyset_i$ represents the AR coefficients, θ_j represent the MA coefficients, ω_t represents the noise and x_t represents the time series values.

B. MIN-MAX NORMALIZATION

Since the features/input variables in this study differ from one another with regards to the scale, distribution and measurement units, they have to be normalized before they are used by the deep learning LSTM networks. This is done inroder to prevent a model being too sensitive to changes within the input data and big weight values which can singnificantly hamper the training process [13]. A min-max normalization algorithm described by equation (3) is used in this study.

$$\frac{x_i - \min(x)}{\max(x) - \min(x)} \tag{3}$$

where, x_i represents the time series values, min(x) represents the value with the smallest magnitude in the data and max (x) represents the value with the biggest value in the data.

FIGURE 7. 317 kWp solar PV power plant in Bialystok, poland.

C. SLIDING WINDOW ALGORITHM

The LSTM models require the data to be resphaed in the form of [samples, timesteps, features]. This is the motivation for using the sliding window algorithm shown in Algorithm 1. It is making a scan across the length of the input data and reconfigures it so that it can be fed as an input to the LSTM model for training and also making predictions. Without the sliding window the LSTM model while usage will produce an error.

Algorithm 1 Sliding Window Algorithm

1: Initialize variables (Y, C); where Y is the total length of the time series and C is the sliding window length
2: j = 0, m = 0; where j represents the time step count at every iteration i and m is the sliding window count
3: W = []; is the array containing extracted windows
4:**While**
 j + C ≤ length (Y); checks if the length of the time series data is not exceeded while extracting windows
 W[n] = Y[i.... (i + C – 1)]; extracts a window from the time series at every iteration and saves it in W
 j = j + C; m = m + 1; increase the time step count by the window size at every iteration and increase the window number by 1
5: **end While**

D. DATA DESCRIPTION

The data for this study is obtained from a metallurgical company that is located in the noth east of Poland in the city of Bialystok close to the Lithuanian border.

The factory associated with the company is involved in high grade stainless steel production for car accessories and has an annual energy cosumption that has been steadily increasing from 0.531 MWh in 2018 to 1.190 MWh in the year 2021. In order to move towards a carbon neutral scenario and also participate in electricity markets to improve flexibility of the entire installation a 317 kW peak power solar PV plant was set up as shown in Fig. 7. Recently, the company decided to participate in the ERA-NET project MESH4U from the industrial partner side for the purpose of exploring efficient solar and load forecasting methods of which the solar forecasting part is presented in this paper.

The two variables also called as features for the forecasting problem are shown in Fig. 8. The first subplot shows the PV power output in Watts from the Januray 2014 to January 2019 whereas the second subplot provides irradiation for the same time frame in W/m^2. In both cases the seasonal trend can be clearly observed where both the output power and the irradiation values peak during the summer months around july and plummet during the winter months around January.

IV. EVALUATION METRICS

For this study the evaluation metrics chosen were the Root Mean Squared Error (RMSE), the Mean Bias Error (MBE) and the Mean Absolute Error (MAE). These 3 metrics were chosen particularly as it was recommended by highly cited papers and an International Energy Agency (IEA) report on solar forecasting [24], [25], [26]. The MAE is the most straightforward metric since it calculates the absolute value of the error at every time step as shown in (4). The error is simply

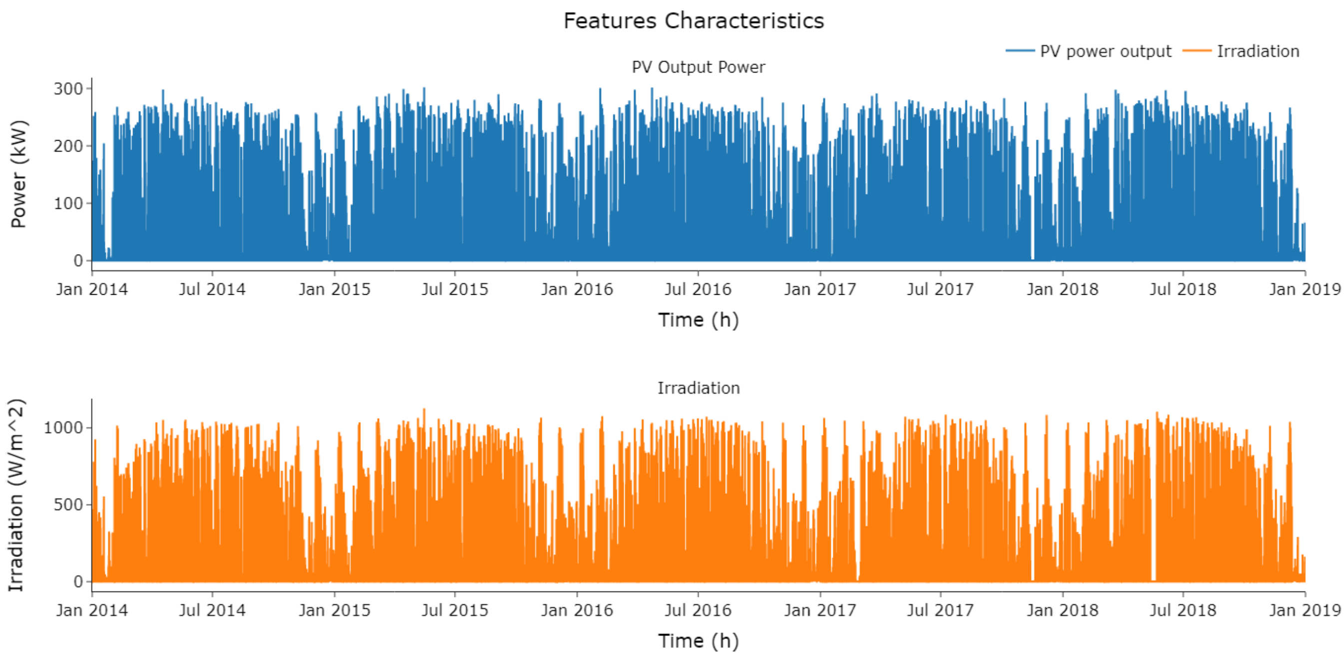

FIGURE 8. **PV output power and irradiation trend.**

the difference between the forecasted and actual value of the target variable at every time step. The RMSE is different from the MAE in the fact that it has the ability to punish the greater errors with the greatest effect and the smaller errors with a lesser effect. It is calculated by averaging the sum of the sqaured absolute error values at each time step and taking its root. It is mathematically shown in (5). The MBE is a metric that does not work with the absolute values as its purpose is to observe on an average if the forecasting algorithm has the tendency to overpredict or underpredict. It is calculated as shown in (6) and the error is calcuated as shown in (7).

$$MAE = \frac{1}{N}\sum\nolimits_{i=1}^{N} |e_i| \tag{4}$$

$$RMSE = \sqrt{MSE} = \sqrt{\frac{1}{N}\sum\nolimits_{i=1}^{N} e_i^2} \tag{5}$$

$$MBE = \frac{1}{N}\sum\nolimits_{i=1}^{N} e_i \tag{6}$$

$$e_i = y_{i(forecast)} y_{i(actual)} \tag{7}$$

where, e_i represents the error calculated in each time step i from the forecasted variable $y_{i(forecast)}$ and the actual variable value $y_{i(actual)}$.

V. RESULTS

A. STATISTICAL ANALYSIS

Since the LSTM models considered vary in performance from one run to another it is imperative to establish reliability of the models by making a statistical analysis. For this reason, each of the 4 models were run a hundred times where every time randomly sampled parts of the input data were used for training and testing. For the vanilla model the results are presented in Table 1. It can be seen that the mean RMSE value for the model is 15.72 kW for a 317 kW PV power plant which represents 4.9% of the peak power value and the mean MAE value is 8.30 kW which is 2.6% of peak value. The 95% confidence interval for the RMSE and MAE have a width of 3.42 kW and 1.78 kW which are 1% and 0.5% of the peak power. This analysis shows the consistency of the vanilla model in making accurate forecasts since the error metrics for 95% of the 100 runs are restricted to a small range.

TABLE 1. **Vanilla LSTM statistical metrics.**

Metric	Minimum (kW)	Mean (kW)	Maximum (kW)	95% confidence interval (kW)
RMSE	0.06	15.72	38.67	[14.01 – 17.43]
MAE	0.06	8.30	18.25	[7.41 – 9.13]

Table 2 presents the statistical test results for the stacked LSTM model. It can be observed that the mean RMSE value at 14.39 kW signifies 4.5% of the peak power value and the MAE at 7.79 kW at 2.4 % of the same. The 95% confidence interval has a width of 0.9% of the peak power value for the RMSE and 0.5% of the same for the MAE. These results show a slight improvement in both accuracy and reliability compared to the LSTM vanilla model.

TABLE 2. **Stacked LSTM statistical metrics.**

Metric	Minimum (kW)	Mean (kW)	Maximum (kW)	95% confidence interval (kW)
RMSE	0.06	14.39	30.11	[12.87 – 15.85]
MAE	0.06	7.79	15.72	[6.97 – 8.62]

Table 3 shows that the Bi-directional LSTM has a mean RMSE and MAE value of 12.87 and 6.91 respectively which amount to 4% and 2.1% of the peak power. Moreover, the confidence interval for both the RMSE and MAE have a width of 0.8% and 0.5% of the peak power respectively. This shows that the Bi-directional model is slightly more accurate than both the Vanilla and Stacked models but it is similar in reliability to the Stacked model.

TABLE 3. Bi-directional LSTM statistical metrics.

Metric	Minimum (kW)	Mean (kW)	Maximum (kW)	95% confidence interval (kW)
RMSE	0.06	12.87	30.30	[11.53 – 14.20]
MAE	0.06	6.91	16.16	[6.657 – 8.43]

Table 4 for the LSTM-Autoencoder model shows that it has a mean RMSE and MAE value of 15.59 and 8.36 respectively which amount to 4.9% and 2.6% of the peak power. Moreover, the confidence interval for both the RMSE and MAE have a width of 0.5% and 0.5% of the peak power respectively. This shows that the LSTM-Autoencoder model is slightly less accurate than both the Bi-directional and Stacked models, but it is the most reliable of all models due to smaller width of the confidence intervals.

TABLE 4. LSTM-Autoencoder statistical metrics.

Metric	Minimum (kW)	Mean (kW)	Maximum (kW)	95% confidence interval (kW)
RMSE	0.31	15.59	39.94	[13.88 – 17.20]
MAE	0.31	8.36	22.25	[7.48 – 9.25]

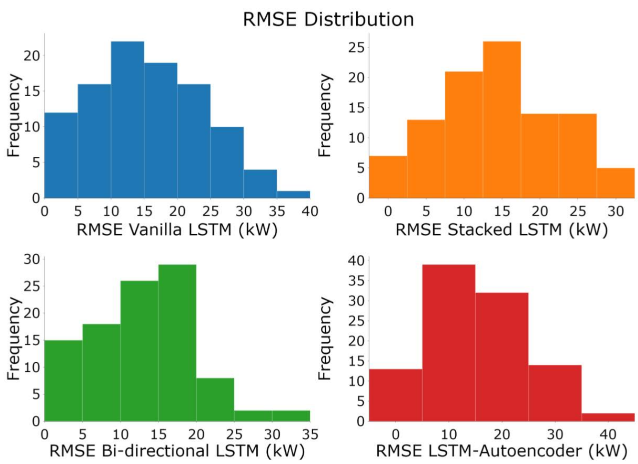

FIGURE 9. RMSE distributions.

The RMSE and the MAE frequency plots for all the investigated algorithms run for 100 times are shown in Fig. 9 and Fig. 10 respectively. For the RMSE distribution it can be seen that for the Vanilla and Stacked it follows nearly the shape of a normal distribution whereas for the LSTM – Autoencoder model it is more prominent. Similar observations can also be seen with the MAE distributions indicating that the error metrics not only stay within a small range of the peak PV power but are also normally distributed within it. Table 5 presents a comparison of the results of this study with the results obtained from highly cited literature. A direct comparison of the results may not be fair since the regions in comparison are climatically different as countries like Malaysia and Australia have a smaller yearly range in temperature as compared to Poland. Nevertheless, they provide an insight into the performance of the model against popular models that are available. It can be seen that the LSTM – Autoencoder model has a comparable performance to the best models obtained from the literature even though the accuracy metrics of some of the compared models are better. The RMSE was chosen as the metric to be compared since it was commonly used in all the referred articles. Moreover, the percentage of RMSE of the peak power installed capacity was used since the PV panels used for forecasting the studies were of different capacities.

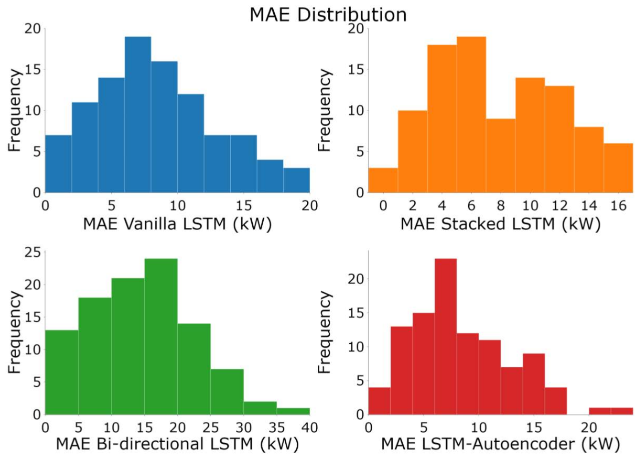

FIGURE 10. MAE distributions.

TABLE 5. Comparison with results from the literature.

Algorithms	Country	RMSE (% of peak power)
RNN – LSTM	Malaysia	1.41%
GASVM	Australia	0.38%
SVM	Australia	22.69%
DEPSO	Australia	4.4%
LSTM – Autoencoder	**Poland**	**4.9%**

B. COMPARISON OF POINT FORECASTS

Before interval forecasts are made with the best performing model. This section presents a visualized compariosn of the forecasting models on major seasons observed in the region. These days were randomly selected from a dataset that wasn't shown to the models during training. In Fig. 11 it can be

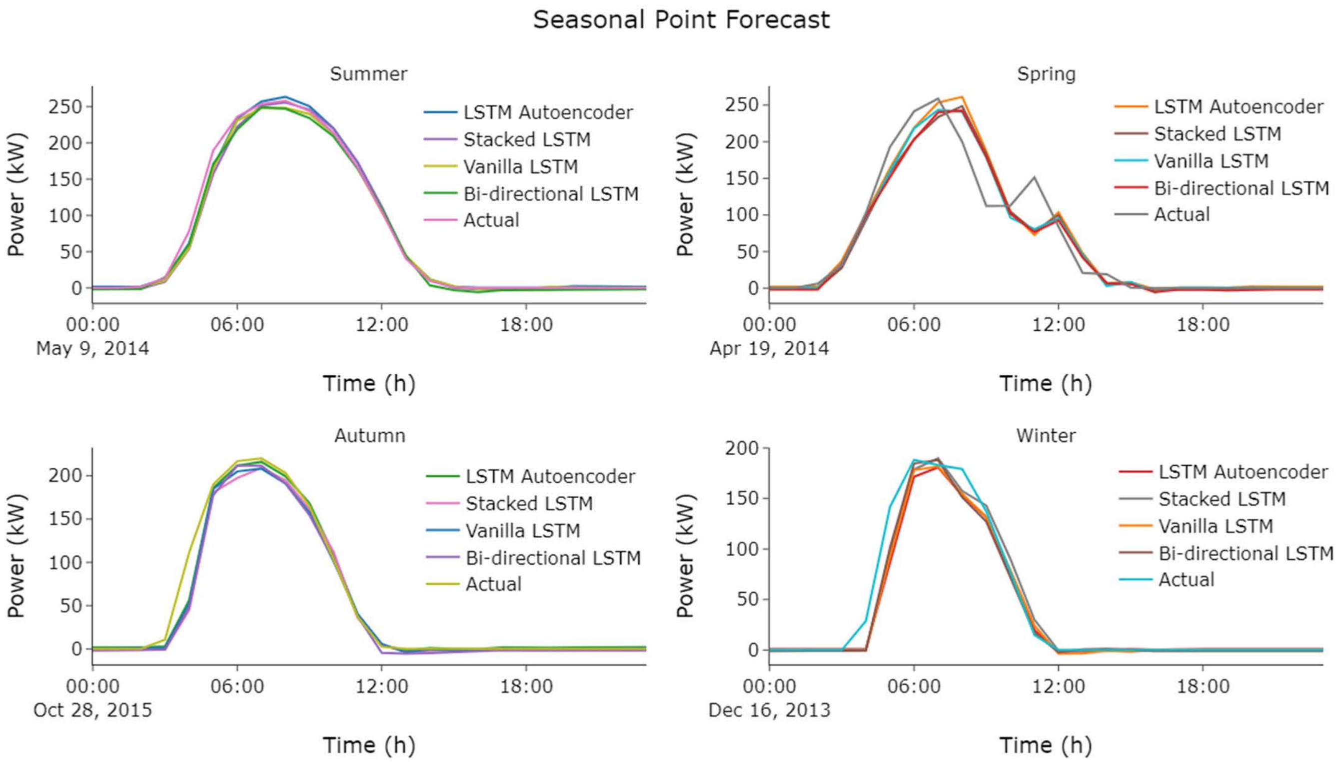

FIGURE 11. Point forecast comparison of all investigated models for random days of every season.

seen that the day representing the summer is the 9th of May. It can be clearly observed that the solar PV panels work much longer in this day when compared to the days in winter and autumn and also the peak power during the day is higher when compared to the others. The forecasting models work well in this example with the forecasting models almost merging with the actual value. The Vanilla LSTM, Stacked LSTM and

Bi-directional LSTM models underpredict whereas the LSTM Autoencoder model overpredicts. The second day representing spring is the 19th of April during which the output remains quite high close to a peak 250 kW and the day is long when compared to the autumn and winter. It can be observed that in this case the forecasting models do not follow the actual value as close as in the summer. This can be attributed to the fact that compared to the summer during the spring there are moments when the sunlight does not reach the solar panels due to significant cloud movement. This results in minor peaks and troughs in the output power characteristic during which achieving high accuracy can be difficult.

The third day concerning the 28th of October represents the autumn season and it can be seen that the peak power is restricted around 200 kW which is much less than the 317 kW installed peak power. In this particular day it can be seen that the forecasts follow the actual value quite closely. This is also because the concerned day does not have any dramatic changes in its characteristic even though such changes do occur during the autumn season just like in the spring season. All the investigated models seem to underpredict in this example and looking closely it can be noticed that the LSTM autoencoder forecasts are the closest to the actual value.

The 4th day representing winter is the 16th of December. During this day it can be seen that the peak power is well below 200 kW. The forecasted models follow the actual model with a good degree of accuracy despite minor abrupt changes in the characteristic. All the explored models underpredict for most of the day with the LSTM autoencoder seeming more accurate than the other models.

C. SEASONAL INTERVAL FORECASTS FOR THE LSTM-AUTOENCODER MODEL

Fig. 12 presents the seasonal interval forecasts made by the LSTM-Autoencoder model. Finally, this model was selected due to its reliability which can be seen from the width of its 95% confidence interval from running it over 100 times. This decision was made because the difference in accuracy between the models and the reliability is quite small but from the electricity market point of view having reliable information is more important than a slight benefit on accuracy.

The days were once again picked in random from different seasons observed in the region. These days are different from the ones used in Fig. 12 and for the summer the 28th of August was chosen which is at the end of the summer season for the region. It can be observed that the forecasts made by the LSTM-Autoencoder model stay within the forecast +/- the 95% confidence interval for the RMSE observed from table 6. The upper and lower bound of the envelope provides further

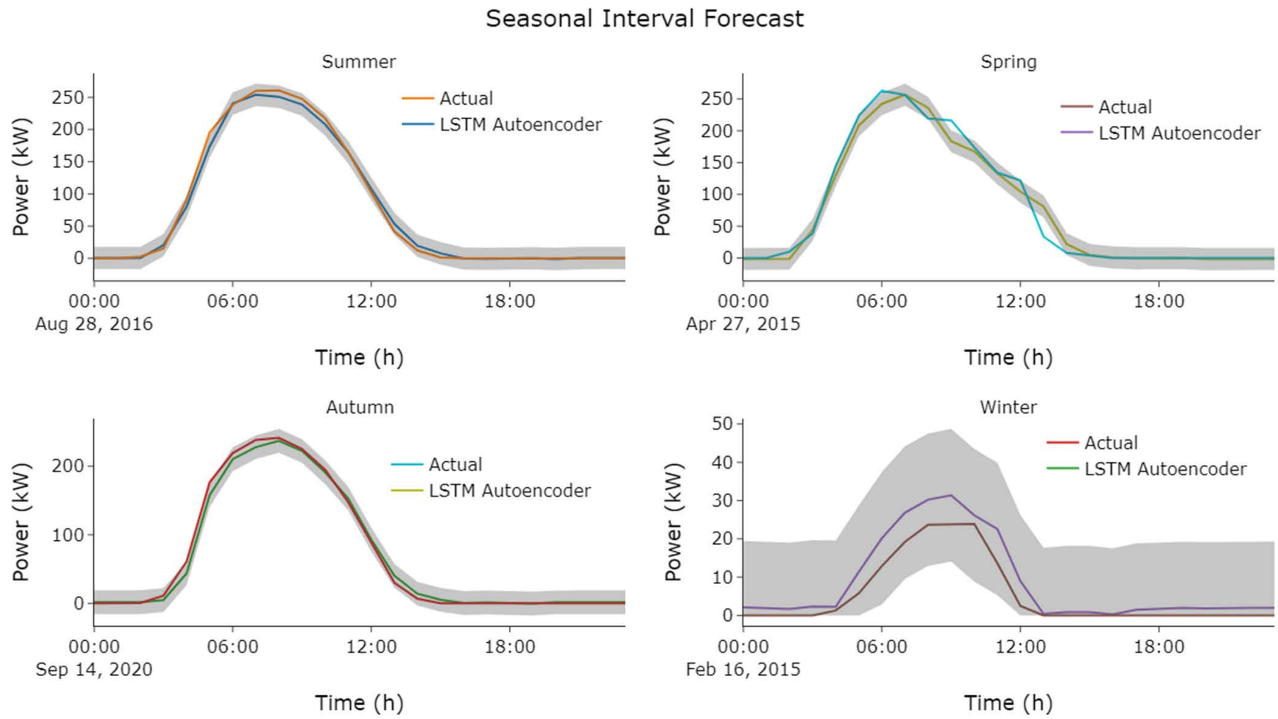

FIGURE 12. Point forecast comparison of all investigated models for random days of every season.

information that can be useful in decision making regarding electricity market participation and planning. The idea is that in general 95% of the forecasts made will fall within this region of error above and below the forecast. 27th. of April representing the spring season is a day of fluctuations and it can be seen that two data points in fact lie outside the confidence intervals and such a behavior is seen during days of high fluctuations which cannot be avoided. Nevertheless, the other observations do fall within the envelope. For the 14th of September representing the autumn season it can be noticed that the day is quite regular without any sudden increases or fall in output power and the accuracy remains high with all actual values falling within the 95% confidence intervals.

For the winter day of 16th February, it can be seen that it is a day of very low power output. The peak power of the day is 30 kW which is about 10% of the peak power capacity of the solar PV power plant. From the figure it can be seen that the forecast is quite accurate with a deviation of only a few kilowatts for such a big power plant. It can be seen that the actual value stays completely within the confidence.

Despite the above results the shortcomings of the probabilistic LSTM-Autoencoder can be summarized as follows:

- The current article uses a statistical approach derived from the normal distribution of errors to build forecast intervals. While this approach is easy to implement it produces static intervals which fails to adapt forecast interval sizes during periods of high volatility.
- The current LSTM Autoencoder model is built on results obtained over 100 runs of the same model on different parts of the input and test data. While this approach is comprehensive better results can be
- obtained by running the model in such a manner for 1000 or 10,000 runs. This proposed increased in runs also significantly increases the computational burden.
- Finally, the model described in this paper is trained over a large dataset which is a necessary condition for deep learning models such as the LSTM. It can be concluded that a lack of sufficient data will reduce the performance of the LSTM based forecaster.

VI. CONCLUSION

This paper presents an investigation into 4 different LSTM models for the purpose of hourly ahead solar power output forecasting for a grid connected solar PV plant. From the statistical analysis of the best performing model, a probabilistic forecasting system was created in order to improve decision making when it comes to electricity market participation by the PV plant owner. It was noticed that out of all the models the LSTM Autoencoder model was the most consistent hence, it was selected over the other models as consistency is prioritized by the user over the small accuracy advantages that is provided by the LSTM Bi-directional model.

The performance of the models was compared by looking at different days selected from different seasons that are prevalent in the region and the probabilistic forecasts by the LSTM autoencoder model were also analyzed for other days that were chosen from the different seasons. It was seen that over a 100 runs the LSTM Bi-directional model was the most accurate but the LSTM autoencoder model was the most consistent as width of the 95% confidence intervals for both the RMSE and MAE was 0.5%. Moreover, the error distribution from all the runs was the closest to that of the normal distribution for the LSTM autoencoder model.

The presented work can be improved in several ways. The probabilistic approach employed for the LSTM models in this study is quite simplistic in nature though easy to implement and having low computational burden. The future work includes exploring other possible approaches such as adaptive conformal predictions for time series and bootstrapping approaches. Evaluation of the proposed models against solar power output data from different continental regions to obtain a more generalized result than the current location specific result.

ACKNOWLEDGMENT

This research uses data provided by Alu-Frost Company, Sowlany, Poland (Podlasie Voivodeship), the industry partner of the project, location of the project demonstrator. The collection of the data under the supervision of the project leader Electrum Ltd. Białystok, Poland (Podlasie Voivodeship).

REFERENCES

[1] I. Kougias, N. Taylor, G. Kakoulaki, and A. Jäger-Waldau, ''The role of photovoltaics for the European green deal and the recovery plan,'' *Renew. Sustain. Energy Rev.*, vol. 144, pp. 1–8, Mar. 2021, doi: 10.1016/J.RSER.2021.111017.

[2] E. Comission, ''The European green deal,'' Eur. Commission, Brussels, Belgium, Tech. Rep. COM(2019)640, 2019.

[3] R. Tawn and J. Browell, ''A review of very short-term wind and solar power forecasting,'' *Renew. Sustain. Energy Rev.*, vol. 153, Jan. 2022, Art. no. 111758, doi: 10.1016/j.rser.2021.111758.

[4] R. Ahmed, V. Sreeram, Y. Mishra, and M. D. Arif, ''A review and evaluation of the state-of-the-art in PV solar power forecasting: Techniques and optimization,'' *Renew. Sustain. Energy Rev.*, vol. 124, May 2020, Art. no. 109792, doi: 10.1016/j.rser.2020.109792.

[5] P. Singla, M. Duhan, and S. Saroha, ''A comprehensive review and analysis of solar forecasting techniques,'' *Frontiers Energy*, vol. 16, no. 2, pp. 187–223, Apr. 2022, doi: 10.1007/s11708-021-0722-7.

[6] X. Qing and Y. Niu, ''Hourly day-ahead solar irradiance prediction using weather forecasts by LSTM,'' *Energy*, vol. 148, pp. 461–468, Apr. 2018, doi: 10.1016/j.energy.2018.01.177.

[7] M. N. Akhter, S. Mekhilef, H. Mokhlis, Z. M. Almohaimeed, M. A. Muhammad, A. S. M. Khairuddin, R. Akram, and M. M. Hussain, ''An hour-ahead PV power forecasting method based on an RNN-LSTM model for three different PV plants,'' *Energies*, vol. 15, no. 6, p. 2243, Mar. 2022, doi: 10.3390/en15062243.

[8] T. Zhu, Y. Guo, Z. Li, and C. Wang, ''Solar radiation prediction based on convolution neural network and long short-term memory,'' *Energies*, vol. 14, no. 24, p. 8498, Dec. 2021, doi: 10.3390/en14248498.

[9] P. Singla, M. Duhan, and S. Saroha, ''A hybrid solar irradiance forecasting using full wavelet packet decomposition and bi-directional long short-term memory (BiLSTM),'' *Arabian J. Sci. Eng.*, Mar. 2022, doi: 10.1007/s13369-022-06655-2.

[10] V. D. William, ''Short-term PV power forecasting using hybrid GASVM technique,'' *Renew. Energy*, vol. 140, pp. 367–379, Feb. 2019, doi: 10.1016/j.renene.2019.02.087.

[11] U. K. Das, K. S. Tey, M. Seyedmahmoudian, S. Mekhilef, M. Y. I. Idris, W. Van Deventer, B. Horan, and A. Stojcevski, ''Forecasting of photovoltaic power generation and model optimization: A review,'' *Renew. Sustain. Energy Rev.*, vol. 81, pp. 912–928, Jan. 2018, doi: 10.1016/j.rser.2017.08.017.

[12] M. Seyedmahmoudian, E. Jamei, G. Thirunavukkarasu, T. Soon, M. Mortimer, B. Horan, A. Stojcevski, and S. Mekhilef, ''Short-term forecasting of the output power of a building-integrated photovoltaic system using a Metaheuristic approach,'' *Energies*, vol. 11, no. 5, p. 1260, May 2018, doi: 10.3390/en11051260.

[13] V. Suresh, P. Janik, J. M. Guerrero, Z. Leonowicz, and T. Sikorski, ''Microgrid energy management system with embedded deep learning forecaster and combined optimizer,'' *IEEE Access*, vol. 8, pp. 202225–202239, 2020, doi: 10.1109/access.2020.3036131.

[14] M. Abdel-Nasser and K. Mahmoud, ''Accurate photovoltaic power forecasting models using deep LSTM-RNN,'' *Neural Comput. Appl.*, vol. 31, no. 7, pp. 2727–2740, Oct. 2019, doi: 10.1007/s00521-017-3225-z.

[15] Y. T. Wu, M. Yuan, S. Dong, L. Li, and Y. Liu, ''Remaining useful life estimation of engineered systems using vanilla LSTM neural networks,'' *Neurocomputing*, vol. 275, pp. 167–179, Jan. 2018, doi: 10.1016/j.neucom.2017.05.063.

[16] T. Zhang, K. Zhang, and J. Wu, ''Multi-modal attention mechanisms in LSTM and its application to acoustic scene classification,'' in *Proc. Interspeech*, Sep. 2018, pp. 3328–3332, doi: 10.21437/Interspeech.2018-1138.

[17] Y. Kim, K. Seo, R. J. Harrington, Y. Lee, H. Kim, and S. Kim, ''High accuracy modeling for solar PV power generation using noble BD-LSTM-based neural networks with EMA,'' *Appl. Sci.*, vol. 10, no. 20, p. 7339, Oct. 2020, doi: 10.3390/app10207339.

[18] M. Konstantinou, S. Peratikou, and A. G. Charalambides, ''Solar photovoltaic forecasting of power output using LSTM networks,'' *Atmosphere*, vol. 12, no. 1, p. 124, Jan. 2021, doi: 10.3390/atmos12010124.

[19] R. Al-Hajj, A. Assi, and M. M. Fouad, ''Multi-level stacking of long short term memory recurrent models for time series forecasting of solar radiation,'' in *Proc. 10th Int. Conf. Renew. Energy Res. Appl. (ICRERA)*, Sep. 2021, pp. 71–76, doi: 10.1109/ICRERA52334.2021.9598652.

[20] A. Dairi, F. Harrou, Y. Sun, and S. Khadraoui, ''Short-term forecasting of photovoltaic solar power production using variational auto-encoder driven deep learning approach,'' *Appl. Sci.*, vol. 10, no. 23, p. 8400, Nov. 2020, doi: 10.3390/app10238400.

[21] N. Andrew, ''Machine learning yearning, technical strategy for AI engineers in the era of deep learning,'' Tech. Rep., 2018.

[22] H. Demirhan and Z. Renwick, ''Missing value imputation for short to mid-term horizontal solar irradiance data,'' *Appl. Energy*, vol. 225, pp. 998–1012, Sep. 2018, doi: 10.1016/j.apenergy.2018.05.054.

[23] K. Benmouiza and A. Cheknane, ''Small-scale solar radiation forecasting using ARMA and nonlinear autoregressive neural network models,'' *Theor. Appl. Climatol.*, vol. 124, nos. 3–4, pp. 945–958, May 2016, doi: 10.1007/s00704-015-1469-z.

[24] L. Luukkonen, P. Bateman, P. Hiscock, J. Poissant, and Y. Dignard-Bailey, ''Photovoltaic and solar forecasting: State of the art,'' Int. Energy Agency, Paris, France, Tech. Rep. IEA-PVPS T14-01:2013, Oct. 2013.

[25] D. Yang, J. Kleissl, C. A. Gueymard, H. T. Pedro, and C. F. Coimbra, ''History and trends in solar irradiance and PV power forecasting: A preliminary assessment and review using text mining,'' *Sol. Energy*, vol. 168, pp. 60–101, Jul. 2018.

[26] V. Suresh, P. Janik, J. Rezmer, and Z. Leonowicz, ''Forecasting solar PV output using convolutional neural networks with a sliding window algorithm,'' *Energies*, vol. 13, no. 3, p. 723, Feb. 2020, doi: 10.3390/en13030723.

VISHNU SURESH (Member, IEEE) received the B.Tech. degree in power systems from the University of Petroleum and Energy Studies, Dehradun, India, in 2014, the M.S. degree in control in electrical power engineering from the Wroclaw University of Science and Technology, Wroclaw, Poland in 2016, where he received the doctoral degree in microgrid energy management systems with deep learning forecasters and hybrid optimizers, in 2021. In 2021, he was an Associate Scientist at the Embedded Power Systems Department, HITACH ABB Power Grids Research and Development Center, Krakow. He participated as a Guest Researcher for research in microgrids at the Centre, Aalborg University, Aalborg, Denmark. Currently, he is as an Assistant Professor with the Faculty of Electrical Engineering, Wroclaw University of Science and Technology. His current research interests include designing energy management systems for microgrids entailing the use of deep learning-based forecasting algorithms and meta-heuristic/hybrid optimization algorithms.

FACHRIZAL AKSAN (Student Member, IEEE) received the B.Sc. degree in applied science from the State of Polytechnic Ujung Pandang, Indonesia, in 2016, and the M.Sc. degree in renewable energy system from the Wroclaw University of Science and Technology, Wroclaw, Poland, in 2021, where he is currently pursuing the Ph.D. degree with the Faculty of Electrical Engineering. His current research interest includes the forecasting and power management for energy cloud based on the application of deep learning methods.

PRZEMYSLAW JANIK received the M.Sc. and Ph.D. degrees in electrical engineering from the Wroclaw University of Technology, Poland, in 2000 and 2005, respectively. He has been with the Department of Electrical Engineering, Wroclaw University of Technology, since 2002. From 2001 to 2002, he worked at the Dresden University of Technology, Germany. His current research interests include power quality, signal processing, and neural networks.

TOMASZ SIKORSKI (Member, IEEE) received the Ph.D. degree in application of time–frequency analysis in electrical power systems from the Wroclaw University of Science and Technology, Poland, in 2005, and the habilitation degree, in 2014. In 2006, he was a Postdoctoral Researcher at the Laboratory of Brian Science, RIKEN Institute, Tokyo. From 2006 to 2010, he led the postdoctoral project founded by the Polish Ministry of Higher Education and Science dedicated to application of novel signal processing methods in the analysis of power quality disturbances in powers systems with distributed generation. He became a University Professor, in 2016. He cooperates with industry and power system operators on monitoring, detection, and analysis of conducted disturbances and time-varying phenomena in power systems.

B. SRI REVATHI received the B.E. degree in electrical and electronics engineering from Periyar University, India, in 2004, and the M.E. degree in power electronics and drives from Anna University, Chennai, India, in 2006, and the Ph.D. degree in high gain high power DC-DC converters, in 2018. She has about 15 years of teaching and research experience. She is currently an Associate Professor with the School of Electrical Engineering, Vellore Institute of Technology, Chennai, India. She was involved as the Principal Investigator and received the Seed Fund worth Rs.3.4 Lakhs. In February 2022, she received another seed fund for Rs.3 lakhs. She has also received the fellowship from DST-SERB-SIRE, in May 2022. She has published more than 15 journal articles with high impact factor, many conferences and book chapters. Her research interests include high gain high power DC-DC converters, DC microgrids, and machine learning approaches to renewable energy. She is a member of IET and IEI Professional Society.